Research Article
Open Access
Life Sciences, Medicine and Biomedicine

Computational identification of *Melaleuca cajuputi* essential oil compounds targeting *Aedes aegypti* odorant receptors

Muslim Bin Aqeel[1], Tayeb Naeem[1], Shuhaila Mat Sharani[1], Mohd Zulkifli Salleh[2], Mohd Dasuki Sul'ain[1], Zaman Khan[3] & Nurhidanatasha Abu Bakar[1,*]

[1]*Biomedicine Programme, School of Health Sciences, Health Campus, Universiti Sains Malaysia, 16150 Kubang Kerian, Kelantan, Malaysia.*
[2]*Department of Medical Microbiology & Parasitology, School of Medical Sciences, Health Campus, Universiti Sains Malaysia, 16150 Kubang Kerian, Kelantan, Malaysia.*
[3]*Department of Biological and Environmental Sciences, Faculty of Sciences, Emerson University, Multan, Pakistan.*

**Correspondence:* natashaa@usm.my

Received 25 January 2026; Revised 2 June 2026; Accepted 5 June 2026; Published online 8 July 2026

ABSTRACT

Dengue fever is caused by Flaviviridae viruses and transmitted mainly by *Aedes aegypti*; there are about 390 million cases of dengue fever annually, the majority in tropical countries. Increased resistance to insecticides in this vector has reduced the effectiveness of traditional control measures and led to the need for more sustainable alternative control measures using plants. This study aimed to assess the ability of *Melaleuca cajuputi* (cajuput/gelam) essential oil (MCEO) to interfere with the host-seeking behaviour of *Ae. aegypti* by targeting odorant-binding proteins (OdBPs) using a computational approach. 63 OdBP sequences were retrieved from GenBank and homology modeling was done using Swiss-Model, and six MCEO bioactive compounds were retrieved from PubChem and converted from SDF to PDB format using Open Babel GUI. AutoDock Vina was used to evaluate OdBP ligand interactions via molecular docking. After modelling and validation, 14 OdBPs were chosen for analysis for structural reliability, the GMQE values ranged from 0.75-0.89, and more than 85% of the residues were in favoured Ramachandran regions. When docking, strong ligand protein interactions were observed, with OdBP17 having the highest binding affinity for γ-terpinene (−7.4 kcal/mol), interacting with the key residues Leu84, Leu118, Leu129, Phe22, Val68, and Val80. Other significant interactions were found between OdBP39 carene and OdBP27 p-cymene. The values of −6.90 kcal/mol and −8.83 kcal/mol binding affinities to OdBP17 with reference ligands DEET and N-phenyl-1-naphthylamine (NPN), respectively, validated the docking approach in this study. The results show that MCEO compounds can bind with strong affinities to the *Ae. aegypti* OdBPs and can form stable complexes that are potentially functional, which make them promising candidates for natural olfactory disruptors for sustainable control of the dengue vectors.

Keywords: *Aedes aegypti; essential oil; Melaleuca cajuputi; molecular docking simulations and odorant-binding proteins*

INTRODUCTION

Dengue fever is a rapidly spreading, global mosquito-borne disease with no specific treatment currently available. It is caused by the dengue virus from the Flavivirus family and transmitted primarily by the female *Aedes aegypti* mosquito (Herbuela et al., 2019). Each year, an estimated 390 million dengue infections occur worldwide, with Asia accounting for approximately 70% of cases (Bhatt et al., 2013). In 2023, Malaysia reported 111,400 cases, marking the highest global incidence that year (World Health Organization, 2024). This alarming figure can be partly attributed to socio-environmental factors linked to urbanisation and labour migration. The high demand for low-skilled labour in Malaysia attracts many migrant workers, who often live in overcrowded dormitories or informal settlements near their workplaces. Limited access to clean water frequently necessitates water storage in containers, unintentionally creating mosquito breeding grounds (Wahab, 2020). As mosquito populations thrive in these environments, the widespread use

https://doi.org/10.28916/lsmb.10.1.2026.258

of chemical insecticides has become common which has led to the development of resistance, posing a significant challenge to vector control. As a result, there is a renewed global interest in plant-based bioinsecticides, driving efforts to screen and isolate bioactive phytochemicals (Su & Mulla, 1999). These natural compounds are often biodegradable, environmentally friendly, and minimally hazardous to human health. Their complex chemical structures also reduce the likelihood of mosquitoes developing resistance, making them a promising alternative to conventional insecticides.

One key component of an integrated mosquito management strategy is the use of mosquito repellents of natural origins from aromatic plant-derived essential oils, which help reduce mosquito bites and transmission of mosquito-borne diseases (Lina et al., 2025; Xue et al., 2003). Essential oils from plant families such as *Myrtaceae, Lamiaceae, Asteraceae, Fabaceae,* and *Apiaceae* are well-known for their mosquito repellent activity (Mahmud et al., 2019). These oils are produced in the cytoplasm and plastids of plant cells (Mathew & Rothman, 2008) and contain a variety of volatile molecules such as hydrocarbons, oxygenated hydrocarbons, and phenylpropenes. Among these, monoterpenes are the primary active compounds in essential oils (Meerdink, 1989), with compounds such as α-pinene, p-cymene, limonene, terpinolene, eugenol, thymol, camphor, citronellol, and citronellal being responsible for repelling mosquitoes (Montesinos, 2003; Murugesan & Manoharan, 2020). *Melaleuca cajuputi* essential oil (MCEO), commonly known as cajuput oil, is a volatile oil extracted from leaves and twigs of the *M. cajuputi* tree (Noor et al., 2021). The plant is a member of the *Myrtaceae* family native to Southeast Asia and northern Australia, and naturally grows in inland, coastal, and subcoastal regions, as well as along riverbanks. It can grow up to 25 meters tall with a single flexible trunk and various adventitious roots (Doran, 1999). As illustrated in Figure 1, its dark green, lanceolate leaves are silky-hairy and arranged alternately, with prominent oil glands and veins. The petiole is concave-convex, and inflorescences appear singly, or in groups of two or three (Daud et al., 2015; Doran, 1999). The greenish-white flowers are arranged in triads along the stems, with hairy sepals and sub-cylindrical tubules. MCEO is characterised by a clear to pale yellow colour and a sharp, camphoraceous scent. Chemically, it is rich in monoterpenes and sesquiterpenes and contains major bioactive compounds such as 1,8-cineole (eucalyptol), α-terpineol, γ-terpinene, p-cymene, and carene, which are known for their antimicrobial, anti-inflammatory, insecticidal, and repellent activities. Six major bioactive compounds of MCEO were selected based on their reported abundance and biological activity in the chemical composition of MCEO as described in the literature (Noor, 2023; Noor et al., 2021; Majeed et al., 2015). In a series of gas chromatography–mass spectrometry (GC-MS) analyses of MCEO, the following compounds were found as major constituents and selected as representative of the major monoterpene and oxygenated terpene groups present in MCEO: carene, linalool, p-cymene, tyranton, 1,8-cineole, and γ-terpinene. These compounds were chosen for detailed interaction analysis because γ-terpinene, which was one of the most abundant compounds, was reported as an insecticidal and repellent compound (Majeed et al., 2015; Noor, 2023; Noor et al., 2021). Given its promising biological profile, MCEO is gaining attention as a natural alternative to synthetic insecticides, particularly in targeting mosquito vectors like *Ae. aegypti*.

Figure 1

M. cajuputi growing in a forest near a beach in Terengganu, Malaysia

Note: (A) Melaleuca cajuputi growing in a forest near a beach in Terengganu. (B) Leaves of Melaleuca cajuputi. (C) Flower of Melaleuca cajuputi

Ae. aegypti odorant-binding proteins (OdBPs) are small, soluble proteins found in the mosquito's antennae and maxillary palps, where they play a pivotal role in detecting chemical signals, particularly human odours for host-seeking behaviour (Bohbot et al., 2011). Structurally, OdBPs are characterised by a conserved framework of six α-helices stabilised by disulfide bonds formed between conserved cysteine residues, enabling them to efficiently capture, stabilise, and transport odorant molecules to olfactory receptors (Armbruster et al., 2009). This molecular mechanism also governs other essential behaviours such as reproduction and oviposition. Given the central role of OdBPs in the mosquito's olfactory system, interfering with their function presents a promising strategy for vector control. MCEO has the potential to disrupt the mosquito's olfactory-guided host-seeking behaviour, reducing its ability to locate and bite human hosts. This study was designed to explore the potential by evaluating selected compounds from MCEO for their disruption of the OdBPs function in *Ae. aegypti* via in silico computational approach. The molecular docking simulation

was used to predict the binding affinity and the interaction sites between the OdBPs and the MCEO compounds, which could be used as a base for future experimental verification and designing plant-based bioinsecticides

METHODOLOGY

Data acquisition

Sequences of Ae. aegypti odorant-binding proteins

Sequences of *Ae. aegypti* OdBPs in FASTA format were obtained from the GenBank database, with the full list of proteins and their corresponding GenBank IDs compiled in Table 1 as described by Sierra et al. (2021). The UniProtKB database was used to access a total of 63 sequences of odorant binding proteins (OdBP) of *Ae. aegypti*. The sequences are not truncated fragments of the OdBPs, but represent the entire catalogue of full-length OdBPs annotated in the genome of *Ae. aegypti* and were used for downstream structural modelling. Each of these 63 OdBPs has functional differences in its expression patterns in the different parts of the olfactory system (e.g., antennae vs. proboscis), and in its binding specificity preferences for different classes of chemical environmental semiochemicals, enabling the vector to navigate complex olfactory environments. To identify potential inhibitory compounds targeting OdBPs, ligand structures of selected MCEO compounds were sourced from the PubChem database available at https://pubchem.ncbi.nlm.nih.gov/ (Kim et al., 2021). PubChem IDs were used as unique identifiers to ensure reliable access to chemical and biological information for each compound. The selected ligands were downloaded in SDF format and then converted to PDB format using the Open Babel GUI available at (https://openbabel.org/docs/Installation/install.html) (O'Boyle et al., 2011). This conversion was necessary to prepare the ligand structures for molecular docking simulations in the next phase of the study.

Ligand structures of M. cajuputi essential oil compounds

Bioactive compounds of MCEO were retrieved from the PubChem database (https://pubchem.ncbi.nlm.nih.gov/) (Kim et al., 2021) using their unique PubChem IDs to ensure data accuracy (Table 2). Based on literature-reported chemical profiles, six major bioactive compounds of MCEO were selected in this study, including γ-terpinene, which served as a representative compound for further analysis.

Table 1

OdBPs of Ae. aegypti with GenBank IDs (Sierra et al., 2021)

OdBP	Transcript	GenBank ID	Supercontigs position
AaegOdBP1	AAEL006454	EAT41942	1.206:50737:67086:1
AaegOdBP2	AAEL000071	EAT48978	1.1:4056982:4057610: −1
AaegOdBP3	AAEL000051	EAT48979	1.1:4124658:4140143:1
AaegOdBP4	AAEL000073	EAT48980	1.1:4140321:4154466: −1
AaegOdBP5	AAEL000139	EAT48848	1.2:651524:652909: −1
AaegOdBP6	AAEL000821	EAT48127	1.17:3417930:3418697:1
AaegOdBP7	AAEL000833	EAT48136	1.17:3935676:3936843: −1
AaegOdBP8	AAEL001826	EAT47062	1.43:1541221:1541846:1
AaegOdBP9	AAEL002596	EAT46202	1.61:1448858:1449413:1
AaegOdBP10	AAEL007603	EAT40682	1.266:1269968:1270519:1
AaegOdBP11	AAEL002587	EAT46205	1.61:1518773:1519546: −1
AaegOdBP12	AAEL002617	EAT46206	1.61:1525746:1526203:1
AaegOdBP13	AAEL002591	EAT46207	1.61:1541151:1541767: −1
AaegOdBP14	AAEL002605	EAT32319	1.61:1560540:1560999:1

Note: Complete catalogue of Aedes aegypti odorant-binding proteins (OdBPs) retrieved for homology modelling. The table lists all 63 full-length OdBPs annotated in the Ae. aegypti genome, with their corresponding VectorBase transcript identifiers, GenBank accession numbers, and genomic coordinates on supercontigs (adapted from Sierra et al., 2021).

Table 1 (continued)

OdBPs of Ae. aegypti with GenBank IDs (Sierra et al., 2021)

OdBP	Transcript	GenBank ID	Supercontigs position
AaegOdBP15	AAEL002598	EAT46211	1.61:1605563:1618454:1
AaegOdBP16	AAEL003315	EAT45429	1.83:2455477:2456452:1
AaegOdBP17	AAEL004339	EAT44281	1.115:1055155:1055633:1
AaegOdBP18	AAEL004342	EAT44282	1.115:1056506:1057069: −1
AaegOdBP19	AAEL004343	EAT44284	1.115:1059658:1060207: −1
AaegOdBP20	AAEL005778	EAT42712	1.174:827019:827663: −1
AaegOdBP21	AAEL005770	EAT42724	1.174:1511030:1512166:1
AaegOdBP22	AAEL005772	EAT42725	1.174:1532890:1533675:1
AaegOdBP23	AAEL006109	EAT42362	1.189:217057:217969: −1
AaegOdBP24	AAEL006108	EAT42350	1.189:234195:245248:1
AaegOdBP25	AAEL006103	EAT42360	1.189:2037030:2054778: −1
AaegOdBP26	AAEL006106	EAT42362	1.189:2063847:2065664:1
AaegOdBP27	AAEL006176	EAT42273	1.193:1418261:1435259: −1
AaegOdBP28	AAEL006393	EAT42030	1.203:1485149:1497912: −1
AaegOdBP29	AAEL006387	EAT42031	1.203:1497040:1521142: −1
AaegOdBP31	AAEL006396	EAT42032	1.203:1526927:1527922: −1
AaegOdBP32	AAEL006398	EAT42033	1.203:1537009:1538019: −1
AaegOdBP33	AAEL006385	EAT42034	1.203:1538561:1539571: −1
AaegOdBP34	AAEL014082	EAT33639	1.1002:187323:188351:1
AaegOdBP35	AAEL002606	EAT46204	1.61:1497852:1498861:1
AaegOdBP36	AAEL008011	EAT40243	1.294:802739:803197: −1
AaegOdBP37	AAEL008009	EAT40244	1.294:823671:828548: −1
AaegOdBP38	AAEL008013	EAT40246	1.294:1185169:1186628: −1
AaegOdBP39	AAEL009449	EAT38681	1.397:1059780:1064175:1
AaegOdBP40	AAEL009597	EAT38527	1.411:257365:258240:1
AaegOdBP41	AAEL009599	EAT38528	1.411:258377:259352:1
AaegOdBP42	AAEL010666	EAT32309	1.495:848252:848790:1
AaegOdBP43	AAEL010662	EAT37338	1.495:849614:850509:1
AaegOdBP44	AAEL010718	EAT37276	1.500:470519:471178:1
AaegOdBP45	AAEL010714	EAT37277	1.500:485823:486827:1
AaegOdBP46	AAEL010872	EAT37095	1.514:549927:550986: −1
AaegOdBP47	AAEL011499	EAT36414	1.584:253363:254080: −1
AaegOdBP48	AAEL011494	EAT36416	1.584:270443:271204: −1
AaegOdBP49	AAEL011484	EAT36419	1.584:357678:358469: −1
AaegOdBP50	AAEL011490	EAT36420	1.584:358749:359468:1
AaegOdBP51	AAEL011487	EAT36423	1.584:391587:398988: −1

Note: Complete catalogue of Aedes aegypti odorant-binding proteins (OdBPs) retrieved for homology modelling. The table lists all 63 full-length OdBPs annotated in the Ae. aegypti genome, with their corresponding VectorBase transcript identifiers, GenBank accession numbers, and genomic coordinates on supercontigs (adapted from Sierra et al., 2021).

Table 1 (continued)

OdBPs of Ae. aegypti with GenBank IDs (Sierra et al., 2021)

OdBP	Transcript	GenBank ID	Supercontigs position
AaegOdBP52	AAEL011491	EAT36425	1.584:422989:423783:1
AaegOdBP53	AAEL011482	EAT36426	1.584:423953:424743:1
AaegOdBP54	AAEL011481	EAT36427	1.584:434945:435608:1
AaegOdBP55	AAEL012377	EAT35452	1.685:122245:142217: −1
AaegOdBP56	AAEL013018	EAT34778	1.776:429863:431937:1
AaegOdBP57	AAEL000035	EAT48964	1.1:3668288:3668784: −1
AaegOdBP58	AAEL014430	EAT33287	1.1115:141516:14944: −1
AaegOdBP59	AAEL015313	EAT32555	1.1784:37928:38729:1
AaegOdBP60	AAEL015499	EAT32357	1.2733:6977:7459: −1
AaegOdBP61	AAEL015554	EAT46208	1.3221:5993:6448:1
AaegOdBP62	AAEL015566	EAT32308	1.3337:1317:2221: −1
AaegOdBP63	AAEL015567	EAT37337	1.3337:2936:3570: −1

Note: Complete catalogue of Ae. aegypti odorant-binding proteins (OdBPs) retrieved for homology modelling. The table lists all 63 full-length OdBPs annotated in the Ae. aegypti genome, with their corresponding VectorBase transcript identifiers, GenBank accession numbers, and genomic coordinates on supercontigs (adapted from Sierra et al., 2021).

Table 2

Bioactive compounds of MCEO with PubChem IDs (Kim et al., 2021)

Serial number	Compound name	PubChem ID	Chemical formula
1	Carene	26049	$C_{10}H_{16}$
2	Linalool	6549	$C_{10}H_{18}O$
3	p-cymene	7463	$C_{10}H_{14}$
4	Tyranton	31256	$C_6H_{12}O_2$
5	1,8-cineole	2758	$C_{10}H_{18}O$
6	γ-terpinene	7461	$C_{10}H_{16}$

Note: Major bioactive compounds of Melaleuca cajuputi essential oil (MCEO) selected for molecular docking. Compounds were retrieved from the PubChem database using their unique PubChem Compound Identifiers (CIDs) to ensure data accuracy.

Homology modelling, validation, and molecular docking of *Ae. aegypti* OdBPs with MCEO compounds

To characterise the *Ae. aegypti* OdBPs, their domain structures were first analysed using the InterPro database available at https://www.ebi.ac.uk/interpro/ (Hunter et al., 2009) in order to determine family membership, sequence length, and predicted molecular functions. This was followed by homology modelling using Swiss-Model (https://swissmodel.expasy.org/interactive) (Waterhouse et al., 2018) based on FASTA sequences obtained from GenBank (https://www.ncbi.nlm.nih.gov/nuccore). The generated 3D protein structures were validated using Ramachandran plot analysis (Waterhouse et al., 2018) and further visualised using UCSF Chimera (https://www.cgl.ucsf.edu/chimera/download.html) (Pettersen et al., 2021) to assess their stereochemical quality. As no crystallographic structures of the *Ae. aegypti* OdBPs were available in the Protein Data Bank, homology models served as reliable structural alternatives. For molecular docking simulations, protein models were prepared by removing water molecules, adding appropriate charges, and converting ligand structures from PDB to PDBQT. Concurrently, ligand structures, originally in SDF format, were converted into PDB format using Open Babel

(https://openbabel.org/docs/Installation/install.html) (O'Boyle et al., 2011) to ensure compatibility with docking software. Docking simulations were performed using AutoDock Vina and MGL tools (https://ccsb.scripps.edu/mgltools/downloads/) (Rizvi et al., 2013), which utilise the Lamarckian genetic algorithm and Solis & Wets local search approaches to predict binding modes and affinities.

Finally, docking results were analysed in UCSF Chimera to visualise and confirm key molecular interactions. The original 63 OdBP sequences were reduced, through systematic filtration, to 14 candidate proteins, using multi-parametric criteria for sequence quality. In addition to the favourable regions in the Ramachandran plot (>85%), sequences were excluded if they: (i) had incomplete open reading frames or truncated N- or C-termini, which would affect the reliability of the structural model based on the downstream homology alignment; (ii) lacked the characteristic six-cysteine structural motif found in disulfide-rich proteins needed for functional disulfide bridging; or (iii) had a sequence identity with the template lower than 30%, which would affect the reliability of the structural model based on the downstream homology alignment.

The reliability of our molecular docking protocol was demonstrated by further blind docking experiments with two high resolution experimental molecular crystal structures of *Ae. aegypti* odorant-binding proteins (OBPs) deposited in the Protein Data Bank, OBP22 (PDB ID: 6OG0) and OBP1 (PDB ID: 3K1E). These structures were chosen because OBP22 is a well-documented experimental structure that is appropriate for the validation of hydrophobic ligand binding, whereas OdBP1 is very close to the homology models of OBP39. Key MCEO compounds (γ-terpinene and carene), as well as reference ligands (DEET, PubChem CID: 4284 and N-phenyl-1-naphthylamine, NPN, PubChem CID: 7013) were docked into the receptor using AutoDock Vina. This enabled us to directly compare the original homology modelling results with the experimentally determined protein structures.

Grid box parameters

Molecular docking simulations were carried out using blind docking, as no previous parameters were found relative to this study. Proteins and ligands were enclosed within the grid box to ensure optimal docking simulation coverage. Table 3 shows Grid Spacing, Grid Points, and Grid Center parameters used in all OdBPs. For each individual protein target, the designated grid box parameters were maintained consistently across all six ligands.

RESULTS

Homology modelling of *Ae. aegypti* OdBPs was conducted using Swiss-Model simulation tool. A total of 63 OdBP sequences were initially retrieved, and homology models were generated for each OdBP. By structural validation with the help of Ramachandran plot analysis (Figure 3), 14 OdBPs were selected for further analysis in view of their high quality of model. The structural reliability of the selected models was confirmed as they showed high percentage of amino acid residues within favourable zones of the Ramachandran plots, more than 85% of residues were found in the favourable zones in both the Ramachandran plots (Figure 3). These OdBPs have been studied using molecular docking simulation to predict the binding affinity of these OdBPs with the MCEO compounds, which is used to assess the functional relevance of these OdBPs. The docking analysis showed significant interactions with some of the OdBPs with MCEO compounds. Of these, the highest binding affinity was for OdBP17 with γ-terpinene (-7.4 kcal/mol) and it is likely to be a main OBP associated with host-seeking behaviour. These results were further confirmed by the analysis of docking to show that OdBP39 and OdBP8 also exhibited considerable binding interactions with carene and p-cymene, respectively. In OdBP17, γ-terpinene was observed to interact with important amino acid residues such as Leu84, Leu118, Leu129, Phe22, Val68, and Val80, suggesting its potential as an inhibitor of mosquito olfactory function.

Comparison of the binding affinity between *Ae. aegypti* OdBPs and MCEO compounds

Table 4 compares the molecular docking results for six MCEO bioactive compounds and their interactions with 14 modelled OdBPs, focusing on projected binding affinities. The docking simulations indicated that these bioactive compounds had variable binding affinities to OdBPs, with certain compounds exhibiting significantly stronger interactions. Among all proteins tested, in particular, OdBP17 showed strong binding affinities for gamma-terpinene (–7.4 kcal/mol), 1,8-cineole (–7.2 kcal/mol) and linalool (–6.5 kcal/mol). In contrast, the binding of carene (-4.8 kcal/mol), p-cymene (-4.6 kcal/mol) and tyranton (-3.2 kcal/mol) was comparatively weaker, underscoring a distinct structural selectivity profile (Table 5).

Table 3

Grid box parameters for molecular docking simulations in AutoDock Vina

Binding pocket	Grid spacing (Å)	Grid points (X, Y, Z)	Grid center (X, Y, Z) (Å)
OdBP1	0.653	74 x 62 x 66	(-16.009, -17.785, 8.324)
OdBP2	0.464	94 x 98 x 90	(-1.668, 4.881, -11.635)
OdBP8	0.542	108 x 124 x 126	(-1.299, 10.011, 15.109)
OdBP9	0.642	100 x 96 x 118	(-13.019, -9.312, 1.578)
OdBP11	0.994	106 x 94 x 70	(0.602, 25.340, 11.012)
OdBP12	0.719	126 x 126 x 88	(16.345, -2.793, 0.111)
OdBP13	0.719	120 x 96 x 126	(-1.574, -2.287, -20.794)
OdBP15	0.686	114 x 100 x 118	(17.788, 1.725, 17.415)
OdBP17	0.664	112 x 112 x 116	(-7.499, -0.474, -5.773)
OdBP24	1.000	126 x 126 x 126	(5.405, 3.556, -16.471)
OdBP27	1.000	126 x 126 x 126	(4.291, -8.018, -1.938)
OdBP34	0.769	126 x 120 x 126	(4.519, 1.343, -2.605)
OdBP36	1.000	126 x 120 x 126	(6.473, 0.292, 0.082)
OdBP39	0.375	102 x 106 x 116	(8.176, 41.808, 22.222)

Note: Grid box parameters for blind molecular docking simulations performed with AutoDock Vina. Parameters for the 14 selected OdBPs include grid spacing (Å), grid point dimensions (X × Y × Z), and grid center coordinates (X, Y, Z in Å).

Table 4

Comparison of the molecular docking for the selected Ae. aegypti OdBPs against potential M. cajuputi bioactive compounds

OdBP / compound	Carene	Linalool	p-cymene	Tyranton	1,8-cineole	γ-terpinene
OdBP1	-5.8	-5.2	-5.7	-4.0	-5.6	-6.4*
OdBP2	-6.6*	-3.7	-6.2	-3.1	-6.6*	-6.2
OdBP8	-6.1	-5.7	-6.9	-4.0	-5.6	-7*
OdBP9	-6.6*	-4.5	-5.8	-4.1	-6.3	-5.8
OdBP11	-6.2*	-3.8	-5.9	-4.1	-5.8	-5.9
OdBP12	-5.8	-5.1	-5.7	-3.8	-6.0	-6.5*
OdBP13	-6.1	-5.8	-6.3	-4.1	-5.6	-6.6*
OdBP15	-5.8*	-4.7	-5.7	-3.8	-5.2	-5.5
OdBP17	-4.8	-6.5	-4.6	-3.2	-7.2	-7.4*
OdBP24	-6.7*	-3.9	-6.3	-4.6	-6.5	-6.3
OdBP27	-5.3	-3.7	-6.9*	-3.7	-6.4	-6.9*
OdBP34	-5.8	-3.4	-5.9*	-4.1	-5.8	-5.9*
OdBP36	-5.9	-4.8	-5.9	-3.9	-6.1*	-5.8
OdBP39	-7.0*	-3.7	-5.9	-4.1	-6.2	-6.5

Note: Comparison of molecular docking binding affinities (kcal/mol) for 14 selected Ae. aegypti OdBPs against six MCEO bioactive compounds. The asterisk (*) denotes the lowest binding energy (highest predicted binding affinity) for each respective OdBP target.

Table 5

Molecular docking scores and interaction profiles of the 14 selected Ae. aegypti OdBPs complexed with their respective top-scoring Melaleuca cajuputi essential oil bioactive ligands

Serial #	OdBPs #	Top score bound Ligand	Docking score (kcal/mol)	Docking results
1	OdBP1	γ-terpinene	-6.4	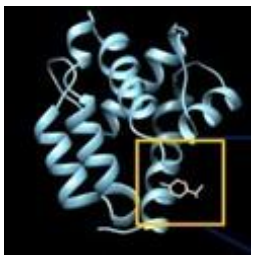 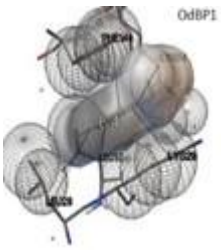
2	OdBP2	Carene / 1,8-cineole	-6.6	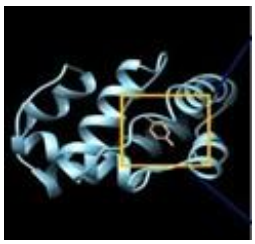 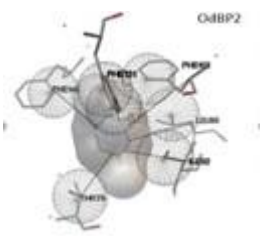
3	OdBP8	γ-terpinene	-7.0	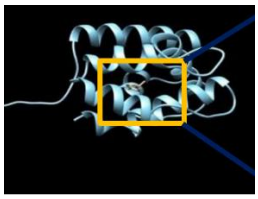 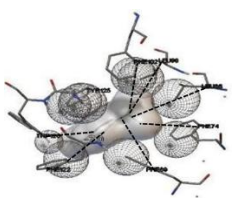
4	OdBP9	Carene	-6.6	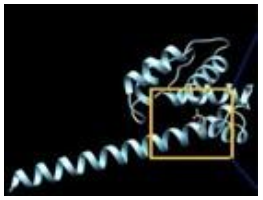 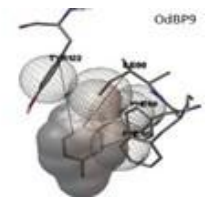
5	OdBP11	Carene	-6.2	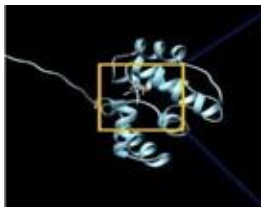 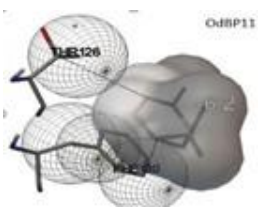
6	OdBP12	γ-terpinene	-6.5	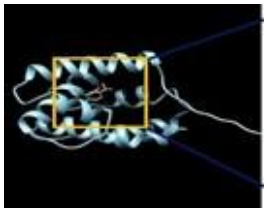 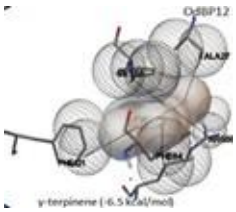

Note: Top-scoring MCEO ligand - OdBP complexes identified from molecular docking simulations. The table presents the best-bound bioactive compound and corresponding docking score (kcal/mol) for each of the 14 selected Ae. Aegypti OdBPs. The asterisk (*) denotes the ligand-receptor complex that demonstrated the absolute lowest binding energy (highest predicted binding affinity) across the entire virtual screening dataset.

Table 5 (continued)

Molecular docking scores and interaction profiles of the 14 selected Ae. aegypti OdBPs complexed with their respective top-scoring Melaleuca cajuputi essential oil bioactive ligands

Serial #	OdBPs #	Top score bound Ligand	Docking score (kcal/mol)	Docking results
7	OdBP13	γ-terpinene	-6.6	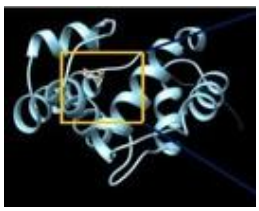 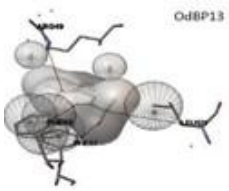
8	OdBP15	Carene	-5.8	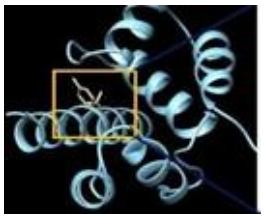 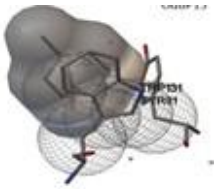
9	OdBP17	γ-terpinene	-7.4*	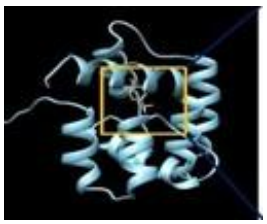 
10	OdBP24	Carene	-6.7	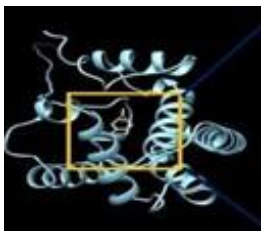 
11	OdBP27	p-cymene / γ-terpinene	-6.9	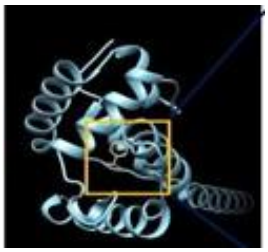 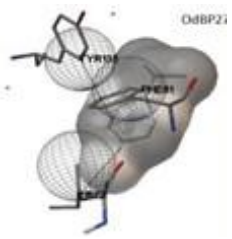
12	OdBP34	p-cymene / γ-terpinene	-5.9	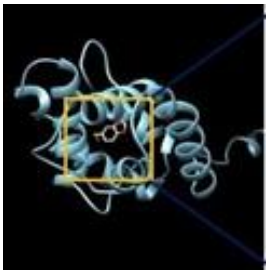 

Note: Top-scoring MCEO ligand - OdBP complexes identified from molecular docking simulations. The table presents the best-bound bioactive compound and corresponding docking score (kcal/mol) for each of the 14 selected Ae. Aegypti

OdBPs. The asterisk (*) denotes the ligand-receptor complex that demonstrated the absolute lowest binding energy (highest predicted binding affinity) across the entire virtual screening dataset.

Table 5 (continued)

Molecular docking scores and interaction profiles of the 14 selected Ae. aegypti OdBPs complexed with their respective top-scoring Melaleuca cajuputi essential oil bioactive ligands

Serial #	OdBPs #	Top score bound Ligand	Docking score (kcal/mol)	Docking results	
13	OdBP36	1,8-cineole	-6.1	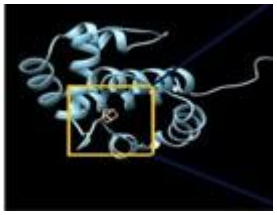	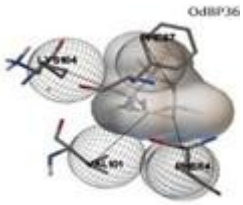
14	OdBP39	Carene	-7.0		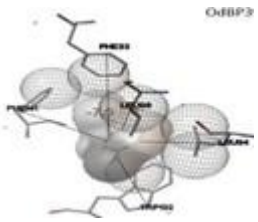

Note: Top-scoring MCEO ligand - OdBP complexes identified from molecular docking simulations. The table presents the best-bound bioactive compound and corresponding docking score (kcal/mol) for each of the 14 selected Ae. aegypti OdBPs. The asterisk (*) denotes the ligand-receptor complex that demonstrated the absolute lowest binding energy (highest predicted binding affinity) across the entire virtual screening dataset.

The parameters of the grid box (Table 3) mirror the structural diversity of the 14 OdBP binding pockets and this directly contributes to the different binding affinities detected in Table 4. Table 3 shows that the size of the grid points and the grid spacing are widely different, resulting in different degrees of approximation of the search volume of the predicted binding cavity (which is a measure of pocket openness and size). OdBP24, OdBP27 and OdBP36 have the highest search volume (grid spacing 1.000 Å; 126 × 126 × 126 to 126 × 120 × 126) and show that the binding cavity is large, open and topologically accessible, thereby allowing a wide variety of ligand topology to be accommodated. OdBP39, on the other hand, shows the smallest and most compact pocket (grid spacing = 0.375 Å; grid points = 102 × 106 × 116), which is also highly geometrically specific, as demonstrated by its highly strong and selective binding to carene (−7.0 kcal/mol). The cavity volume of OdBP17 (112×112×116 grid points, grid spacing 0.664 Å) is in the middle range and is unique due to its highly hydrophobic cavity interior (Table 7), which is composed of only aliphatic amino acid residues (Leu84, Leu118, Leu129, Val68, Val80) and one aromatic residue (Phe22). This is a uniformly non-polar microenvironment which maximises van der Waals contacts and alkyl/pi-alkyl interactions with compact, non-polar monoterpene hydrocarbons, which explains the highest observed binding affinity in the dataset (−7.4 kcal/mol).

The absence of any significant hydrophobic or hydrophilic differences between the binding pockets of OdBP1 and OdBP36 leads to the interesting finding that the two pockets are amphipathic, containing both polar and charged residues that generate localised electrostatic dipoles that are able to interact with the hydrogen bonding network, explaining why the oxygenated monoterpene 1,8-cineole is better accommodated than the purely hydrocarbon ligands. These structural differences, together, form a functional repertoire of OdBP that is able to recognise a wide spectrum of chemical volatiles.

The molecular docking simulation showed that the 14 *Ae. aegypti* OdBPs docked differently with their best *Melaleuca cajuputi* essential oil (MCEO) ligands, with different stabilization structural environments. The complexes are mainly held together by a synergistic combination of strong hydrogen bonding, hydrophobic contacts (alkyl, pi-alkyl) and van der Waals interactions inside the cavities of the internal binding sites, as seen in the high contrast structural figures. The complexes with highest score for example OdBP17 and gamma-terpinene, and OdBP1 and 1,8-cineole, have an optimal steric and geometric fit. For non-polar monoterpene hydrocarbons such as gamma-terpinene, complexed with OdBP17, the stability of the complex is strongly dependent on the hydrophobic network. The non-polar ring is fully buried in a compact hydrophobic patch of residues, allowing the formation of strong alkyl and pi-alkyl interactions,

thereby protecting the ligand from the water surrounding it. The multiple binding modes shown for the major constituents of MCEO indicate that these components can effectively occupy and saturate the functional binding pockets of various *Ae. aegypti* OdBPs by multiple and complementary chemical pathways, providing a good molecular explanation for the biological efficacy of MCEO.

The docking results for both NPN and DEET were validated using the crystal structure of PDB 6OG0 and 3K1E, respectively, which gave a strong binding affinity of -8.83 kcal/mol and -6.90 kcal/mol respectively for both the compounds (Table 7). These values are within the range of binding behaviours seen and depicts the strength of affinities calculated for MCEO compounds on homology models.

The highest binding affinity of *Ae. aegypti* OdBPs based on Ramachandran plots

Table 6 summarises the highest binding affinity observed for each OdBP, along with their structural validation percentage based on Ramachandran plots. These results provide insights into both the strength of binding interactions and the reliability of the protein models. A total of 14 OdBPs were selected and docked with 6 bioactive compounds sourced from the literature. Among these. OdBP17 stood out with the highest binding affinity of -7.4 kcal/mol, demonstrating exceptional ligand-binding capacity. The Ramachandran plot analysis showed that 88.24% residues are in the preferred region and 1.47% residues are in the outlier's region, which indicated a good structural validation. These outliers were mapped and found to be in only flexible regions that are solvent-exposed on the protein surface. Most importantly, there were no outlier-sized residues located within or in the vicinity of the predicted binding sites and/or ligand-binding cavities, which means that the structural domain of the central functional binding pockets is highly trustworthy for molecular docking simulation.

Table 6

Highest binding affinity with validation of homology modelling of OdBPs

OdBP	Highest binding affinity	Ramachandran favoured	Ramachandran outlier
OdBP1	-6.4	99.19	0
OdBP2	-6.6	98.28	0
OdBP8	-7	90.08	3.82
OdBP9	-6.6	98.46	0
OdBP11	-6.2	85.93	2.96
OdBP12	-6.5	89.23	3.08
OdBP13	-6.6	88.46	5.38
OdBP15	-5.8	91.04	5.22
OdBP17	-7.4	88.24	1.47
OdBP24	-6.7	88.38	4.04
OdBP27	-6.9	95.51	0.64
OdBP34	-5.9	97.96	0
OdBP36	-6.1	96.53	0
OdBP39	-7	99.15	0

Note: Highest binding affinity scores and structural validation metrics for the 14 selected OdBP homology models. Ramachandran plot analysis was performed to assess stereochemical quality, reporting the percentage of residues in favoured regions and outlier (disallowed) regions.

OdBP17

InterProScan analysis revealed that OdBP17 belongs to the pheromone/general OdBP protein family, comprising 138 amino acids (Figure 2). To generate a reliable structural model, homology modelling using Swiss-Model was performed with a template based on the AlphaFold DB model of *Ae. albopictus* putative OdBP 56a, which shares a 74.64% sequence identity. The resulting model yielded a GMQE score of 0.87, suggesting high-quality prediction. Among the compounds, γ-terpinene demonstrated the highest binding affinities across several OdBPs, including OdBP1, OdBP8, and OdBP17, with binding affinities up to -7.4 kcal/mol. Molecular docking analysis confirmed that OdBP17 had the

most favourable interaction with γ-terpinene, while tyranton demonstrated the least favourable binding affinity at -3.2 kcal/mol. Detailed interaction analysis revealed that γ-terpinene binds with critical residues in OdBP17, namely Leu84, Leu118, Leu129, Phe22, Val68, and Val80, highlighting its potential as a key modulator of mosquito olfactory pathways (Table 7). Moreover, Binding affinities and the interactions of relevant compounds with OdBP17 is listed in table 8.

Table 7

Computational validation parameters of the canonical Ae. aegypti OBP1 crystal structure (PDB ID: 3K1E) complexed with standard reference controls

Protein (PDB ID)	Ligand	Binding affinity (kcal/mol)	Docking results
OBP22 (6OG0)	NPN (N-phenyl-1-naphthylamine)	-8.83	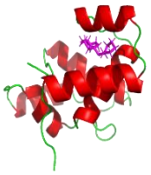
OBP22 (6OG0)	DEET (N,N-Diethyl-meta-toluamide)	-6.90	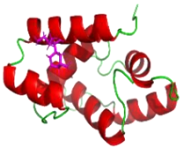
OBP1 (3K1E)	NPN (N-phenyl-1-naphthylamine)	-8.82	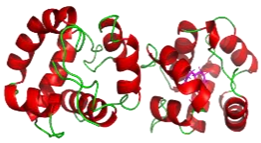
OBP1 (3K1E)	DEET (N,N-Diethyl-meta-toluamide)	-6.90	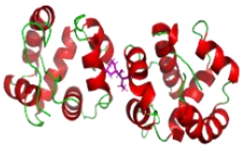

Note: Values represent the top-scoring conformation. The 2D molecular docking diagrams show the ligand-protein binding micro environment. Green residues surround the residues, which suggest van der Waals interactions and C-H bonds, whereas pink/purple residues suggest hydrophobic environments. The intermolecular stabilizing interactions shown are dotted: purple/pink lines indicates alkyl and pi-alkyl hydrophobic bonds interactions, while the green lines represent hydrogen bonding networks that anchor the ligand into the receptor pocket.

DISCUSSION

This research provides compelling evidence that MCEO holds significant promise as a sustainable vector control agent by targeting *Ae. aegypti* OdBPs. Among the bioactive compounds tested, γ-terpinene demonstrated the strongest binding affinity, particularly with OdBP17, where critical residues, Leu84, Leu118, Leu129, Phe22, Val68, and Val80, were involved in stable ligand interactions. The 14 OdBPs selected follow a wide range of binding pocket volumes, shapes, hydrophobicity, and electrostatic character (Table 3), which directly accounts for the observed binding pocket ligand selectivity across the dataset as described in Section 3.1.

Additionally, notable binding interactions were observed for p-cymene with OdBP27 and carene with OdBP39, underscoring the broader relevance of MCEO compounds in disrupting mosquito olfaction. These findings align with earlier studies, such as Bohbot et al. (2011), which emphasised the role of OdBPs in mosquito-host recognition through the detection of human-emitted volatiles. Our results further suggest that the strong interactions between γ-terpinene and OdBP17, and similarly potent interactions with other OdBPs, can be leveraged in developing plant-based alternatives to synthetic pesticides, especially in light of rising insecticide resistance. Moreover, this study demonstrates the value of computational approaches, including homology modelling and molecular docking, in identifying high-affinity interactions for vector control targets. This integrative approach demonstrated the strong potential of MCEO compounds in targeting *Ae. aegypti* OdBPs, thereby supporting their application in mosquito control strategies (Hunter et al., 2009; Kim et al., 2021; Rizvi et al., 2021).

The decision to narrow the analysis from 63 OdBP sequences to 14 based on structural quality allowed for a more precise and meaningful investigation. By focusing on proteins with validated 3D structures, the study enhanced the

reliability of the predicted interactions between OdBPs and MCEO compounds. Plant-based bioactive compounds such as γ-terpinene, p-cymene, and carene continue to show high potential due to their strong binding affinities and eco-friendly properties. This supports earlier reports on essential oils' safety and environmental compatibility compared to conventional chemical insecticides (Su & Mulla, 1999). Notably, ligands with lower affinity, such as tyranton, did not interact with these key residues, further validating the selective binding observed. While previous studies, such as Durofil et al. (2021), recognised γ-terpinene's repellent properties, they lacked a detailed molecular understanding of its interaction with mosquito olfactory proteins.

Table 8

Binding affinity and interactions of compounds with OdBP17

Compounds	Affinity	Interactions
γ-terpinene*	-7.4	LEU84, LEU118, LEU129, PHE22, VAL68, VAL80
1,8-cineole	-7.2	LEU118, PHE122, PHE126, TYR119, VAL68, VAL80
Linalool	-6.5	LEU118, PHE122, 126, VAL 68, VAL80
Carene	-4.8	LEU84, GLU91, GLY91, ALA128
p-cymene	-4.6	LEU84, GLU125, ALA128, VAL87
Safrole	-4.2	LEU84, GLU125, GLN97
Myristicin	-4.1	LEU84, GLU125, VAL87
β-ocimene	-3.9	LEU84, GLU125, LYS124, VAL87
Dillapiole	-3.8	GLU71, ASP70
Tyranton	-3.2	LEU84, GLU88, GLU125

*Note: * represents the highest binding affinities.*

Figure 2

Structure and functional domain analysis of OdBP17

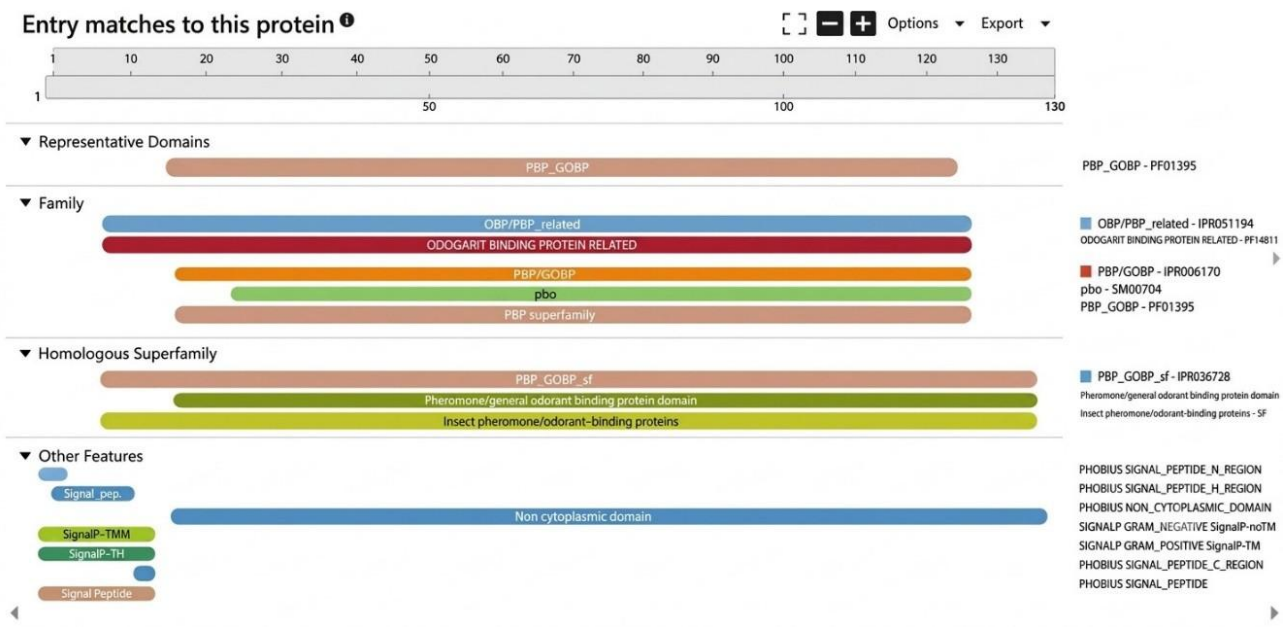

Note: Structural and domain validation of candidate sequences. InterProScan matches correspond directly to the classic insect odorant-binding protein-related family (Family ID: IPR006170), confirming correct target classification.

Figure 3

Ramachandran plot for OdBP17 structure assessment.

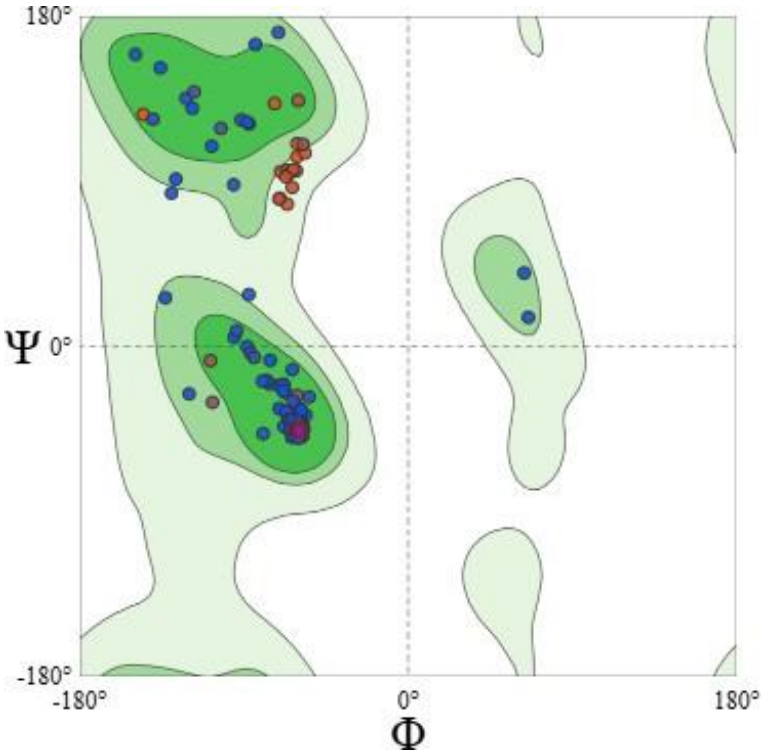

Note: Ramachandran plot for OdBP17 structure assessment. Blue regions depict the residues located within the preferred conformational regions of the Ramachandran plot, whereas red regions indicate residues falling within the outlier regions. The plot confirms that 88.24% of residues reside in favoured regions and 1.47% in outlier regions.

The 14 structures modelled for OdBPs were highly structurally and physiochemically diverse; this is directly reflected in their ligand-binding profiles. The different volumes and topologies, hydrophobicity and electrostatic properties of the cavities generate different microenvironments for different classes of chemicals. For example, the cavity inside of OdBP17 is deeply recessed and sterically shielded, with a hydrophobic aliphatic and aromatic nature, including Leu84, Leu118, Leu129, Phe22, Val68, and Val80. This highly hydrophobic structure allows for maximization of the hydrophobic partition forces and van der Waals contacts that give it an optimal geometry for the compact, non-polar hydrocarbon monoterpenes such as γ-terpinene and p-cymene. In contrast, the pocket surface topography of targets like OdBP1 is more open and amphipathic, with both polar or charged residues (e.g., Lys29, Lys54) and hydrophobic residues (e.g., Leu28, Leu32, Phe144). Such residues create local electrostatic dipoles that can support hydrogen bonding or cation-π interactions that will absorb oxygenated monoterpenes such as 1,8-cineole or linalool. In addition, pockets such as OdBP2 contain dense aromatic networks (Phe103, Phe131 & Phe140) that can provide rigid constraints for stabilising cyclic volatiles.

The structural variation in the OdBP repertoire reflects an evolutionary partitioning of the OdBP periphery. It avoids functional redundancy and enables *Ae. aegypti* to follow complex chemical landscapes by simultaneously discriminating between favourable human host cues (e.g., lactic acid, octenol), oviposition attractants and plant-derived repellent volatiles. Biologically, the fact that the main chemical constituents of MCEO have different chemical geometries with their respective pocket profiles is of great significance from the vector control standpoint. The original system of MCEO is not only to target a single receptor but to flood and “saturate” these separate olfactory pockets. This multi-target competitive inhibition covers up important pathways used by the mosquito to find the host and causes overstimulation of its peripheral nervous system, which accounts for the high levels of repellence and larvicidal activity recorded for essential oils extracted from the plants, as compared to products consisting of individual compounds.

We also further validated our molecular docking protocol with two experimental crystal structures of *Ae. aegypti* OBPs (PDB 6OG0 and 3K1E). As seen in Table 7, NPN had an excellent binding affinity of -8.83 kcal/mol, which is consistent with being a high affinity fluorescent probe, while the DEET had a moderate binding affinity of -6.90 kcal/mol, similar to previous studies that investigated fluorescent displacement (Leal & Leal, 2015; Yin et al., 2015). Most importantly, our top MCEO compounds (γ-terpinene and carene) bound to the homology models in a manner with similar or better binding affinities than the reference compounds, which further confirms their potential as effective disruptors of mosquito olfaction.

Our approach addressed this gap by incorporating rigorous structural validation using Ramachandran plot analysis, which enhances the accuracy and interpretability of molecular docking results. Compared to studies like Sierra et al. (2021), which evaluated mosquito olfactory receptors without extensive model validation, our research presented a more comprehensive computational pipeline that integrated homology modelling, docking, and interaction profiling. Ultimately, this work supports the growing consensus that plant-based bioinsecticides are viable alternatives to synthetic chemical insecticides, particularly in the face of increasing resistance and ecological concerns (Xue et al., 2003; Su & Mulla, 1999). Through a focused, mechanism-based approach, we offered new insights into how MCEO compounds, especially γ-terpinene, can be harnessed to target specific molecular pathways in *Ae. aegypti*, contributing to sustainable and innovative strategies for dengue vector control.

CONCLUSION

Finally, this study offers clear-cut computational proof that *Melaleuca cajuputi* essential oil (MCEO) could be a viable sustainable agent to disrupt the host-seeking behaviour of *Ae. aegypti*, the prime vector of dengue fever via its olfaction. In order to screen the six compounds that were found to be the most bioactive in MCEO in 14 high-quality OdBP models, we used a rigorous homology modelling and blind molecular docking simulation protocol, selecting an initial set of 63 sequences and validating them according to stringent criteria. γ-terpinene was found to be the top ligand with the highest binding affinity in the entire data set, especially towards OdBP17 (−7.4 kcal/mol). The detailed interaction analysis showed that γ-terpinene is deeply embedded in a hydrophobic pocket of OdBP17 with stable van der Waals and alkyl/pi-alkyl interactions with the key residues Leu84, Leu118, Leu129, Phe22, Val68 and Val80. Also noteworthy was the strong interactions between OdBP39 and carene and between OdBP27 and p-cymene, which demonstrate that the efficacy of MCEO is probably due to a multi-target, complementary mode of action, not solely on individual chemical entities.

The results suggest a possible molecular basis for how MCEO was reported to be a repellent and insecticide: the major compounds in MCEO are able to competitively bind to multiple OdBP binding pockets, thereby effectively saturating the peripheral olfactory system of the mosquito, which covers host cues and may lead to neural overstimulation. In addition to making the vector less able to find and bite hosts, this “olfactory saturation” approach also lowers the chances of resistance developing a significant advantage over traditional neurotoxic insecticides, where resistance is becoming more common among *Ae. aegypti* populations. Moreover, being natural compounds extracted from plants, they are environmentally friendly, biodegradable, and can be used in accordance to the global demand for "green" and integrated vector management methods especially in dengue-endemic countries like Malaysia that has an alarmingly high transmission pressure.

Swiss-Model homology modelling, Ramachandran plot validation, and AutoDock Vina docking in the computational pipeline used here gives a solid basis and foundation for their predictions, but we recognize that in silico predictions will need to be confirmed by experimentation. In vitro binding assays, electroantennography and in vivo behavioural trials should be emphasized in future research to confirm the affinities and repellent effect predicted in this screen. If these experimental validations are consistent with our docking results, then γ-terpinene-enriched MCEO formulations will be further developed into new bioinsecticides and/or spatial repellents. In conclusion, the findings of this study align with the emerging evidence of the potential of using plant-based phytochemicals as alternative agents to synthetic pesticides for dengue vector control and public health in tropical and subtropical populations worldwide, providing a path for action that can be taken via the mechanism of action.

The validity of our docking protocol was additionally confirmed with two high-resolution experimental crystal structures of *Ae. aegypti* OBP (6OG0 and 3K1E) to which the reference ligands DEET and NPN had binding energies of −6.90 kcal/mol and −8.83 kcal/mol, respectively. Importantly, several MCEO compounds showed comparable or higher affinities with these references, which indicate their potential to be effective competitive inhibitors of mosquito olfaction. The validity of docking protocol was additionally confirmed with two high-resolution experimental crystal structures of *Ae. aegypti* OBP (−6OG0 and 3K1E) to which the reference ligands DEET and NPN had binding energies of −6.90 kcal/mol and −8.83 kcal/mol, respectively. Importantly, several MCEO compounds showed comparable or higher affinities with these references, which indicate their potential to be effective competitive inhibitors of mosquito olfaction.

The results provide a molecular explanation for the reported peripheral olfactory system multi-target saturation repellent and insecticidal properties of MCEO. MCEO-based compounds are biodegradable, eco-friendly and hold promise as alternatives to chemical insecticides, especially in areas like dengue endemic areas, where resistance is growing. The findings from these in silico studies are promising, but future research with in vitro binding assays, electroantennography and in vivo behavioural testing will help validate these predictions. In summary, this work can enhance the implementation of new approaches to sustainable dengue vector control using plants.

AUTHOR CONTRIBUTIONS

The binding-interaction profiling was conducted by Tayeb Naeem and docking poses/affinity scores were analysed

and figures/visualization were prepared by him. Muslim Bin Aqeel and Mohd Zulkifli Bin Salleh conceived the study and designed the research methodology. Shuhaila Mat Sharani and Nurhidnatasha Abu Bakar helped with the validation of the structural models and interpretation of the molecular interaction data. Dasuki Sulain and Zaman Khan helped in development of the computational workflow, software implementation and technical supervision of the docking protocols. Muslim Bin Aqeel wrote the original draft of the manuscript. The manuscript was critically reviewed and edited by all authors, they participated in the interpretation of the results and agreed to the final manuscript for publication.

ETHICS APPROVAL

Not applicable.

FUNDING

This study was supported by Universiti Sains Malaysia, Short-Term Grant with Project No: R501-LR-RND002-0000000563-0000 and Universitas Andalas, Riset Kolaborasi Luar Negeri with Project No: R504-LR-GAL008-0000000186-U183. The funding body had no role in study design, data collection and analysis, decision to publish or manuscript preparation.

CONFLICT OF INTEREST

The authors declare no conflict of interest in this work.

ACKNOWLEDGEMENTS

We would like to thank all the contributing authors who helped us in this study. This study was supported by Universiti Sains Malaysia, Short-Term Grant with Project No: R501-LR-RND002-0000000563-0000 and Universitas Andalas, Riset Kolaborasi Luar Negeri with Project No: R504-LR-GAL008-0000000186-U183.

REFERENCES

Armbruster, P., White, S., Dzundza, J., Crawford, J., & Zhao, X. (2009). Identification of genes encoding atypical odorant-binding proteins in *Aedes albopictus* (Diptera: Culicidae). *Journal of Medical Entomology*, *46*(2), 271–280. https://doi.org/10.1603/033.046.0211

Bhatt, S., Gething, P. W., Brady, O. J., Messina, J. P., Farlow, A. W., Moyes, C. L., Drake, J. M., Brownstein, J. S., Hoen, A. G., & Sankoh, O. (2013). The global distribution and burden of dengue. *Nature*, *496*(7446), 504–507. https://doi.org/10.1038/nature12060

Bohbot, J. D., Fu, L., Le, T. C., Chauhan, K. R., Cantrell, C. L., & Dickens, J. C. (2011). Multiple activities of insect repellents on odorant receptors in mosquitoes. *Medical and Veterinary Entomology*, *25*(4), 436–444. https://doi.org/10.1111/j.1365-2915.2011.00949.x

Daud, D., Gan, N., Ali, M. T. M., & Tawang, A. (2015). The effect of *Melaleuca cajuputi* methanolic leaves extract on body growth, puberty and sperm quality of juvenile male rats. *Biotechnology-An Indian journal*, *11(9):* 335-339. https://www.tsijournals.com/articles/the-effect-of-melaleuca-cajuputi-methanolic-leaves-extract-on-body-growth-puberty-and-sperm-quality-of-juvenile-male-rat.pdf

Doran, J. C. (1999). Cajuput Oil. In I.Southwell & R. Lowe (Eds), *Tea Tree* (pp. 221-235). CRC Press. https://www.taylorfrancis.com/chapters/edit/10.4324/9780203303603-15/cajuput-oil-john-doran

Durofil, A., Radice, M., Blanco-Salas, J., & Ruiz-Téllez, T. (2021). *Piper aduncum* essential oil: A promising insecticide, acaricide and antiparasitic. A review. *Parasite*, *28*, 42. https://doi.org/10.1051/parasite/2021040

Herbuela, V. R. D. M., De Guzman, F. S., Sobrepeña, G. D., Claudio, A. B. F., Tomas, A. C. V., Arriola-Delos Reyes, C. M., Regalado, R. A., Teodoro, M. M., & Watanabe, K. (2019). Knowledge, attitude, and practices regarding dengue fever among pediatric and adult in-patients in Metro Manila, Philippines. *International Journal of Environmental Research and Public Health*, *16*(23), 4705. https://doi.org/10.3390/ijerph16234705

Hunter, S., Apweiler, R., Attwood, T. K., Bairoch, A., Bateman, A., Binns, D., Bork, P., Das, U., Daugherty, L., & Duquenne, L. (2009). InterPro: the integrative protein signature database. *Nucleic Acids Research*, *37*(suppl 1), D211–D215. https://doi.org/10.1093/nar/gkn785

Kim, S., Chen, J., Cheng, T., Gindulyte, A., He, J., He, S., Li, Q., Shoemaker, B. A., Thiessen, P. A., & Yu, B. (2021). PubChem in 2021: new data content and improved web interfaces. *Nucleic Acids Research*, *49*(D1), D1388–D1395. https://doi.org/10.1093/nar/gkaa971

Leal, G. M., & Leal, W. S. (2015). Binding of a fluorescence reporter and a ligand to an odorant-binding protein of the yellow fever mosquito, *Aedes aegypti*. *F1000Research*, *3*, 305. https://doi.org/10.12688/f1000research.5879.2

Lina, E. C., Aqeel, M. B., Ishak, I. H., Nelly, N., Sulain, M. D., & Bakar, N. A. Mosquito repellents of natural origins from aromatic plant-derived essential oils: A narrative review. *International Journal of Environmental Sciences*, *11*(22s), 2025. https://doi.org/10.64252/3453t436

Mahmud, M. A. F., Abdul Mutalip, M. H., Lodz, N. A., Muhammad, E. N., Yoep, N., Hashim, M. H., Paiwi, F., Rajarethinam, J., Aik, J., & Muhammad, N. A. (2019). Environmental management for dengue control: a systematic review protocol. *BMJ Open*, *9*(5), e026101. https://doi.org/10.1136/bmjopen-2018-026101

Majeed, H., Bian, Y. Y., Ali, B., Jamil, A., Majeed, U., Khan, Q. F., & Fang, Z. (2015). Essential oil encapsulations: Uses, procedures, and trends. *RSC Advances*, *5*, 58449–58463. https://doi.org/10.1039/C5RA06556A

Mathew, A., & Rothman, A. L. (2008). Understanding the contribution of cellular immunity to dengue disease pathogenesis. *Immunological Reviews*, *225*(1), 300–313. https://doi.org/10.1111/j.1600-065X.2008.00678.x

Meerdink, C. L. (1989). Organophosphorus and carbamate insecticide poisoning in large animals. *Veterinary Clinics of North America: Food Animal Practice*, *5*(2), 375–389. https://doi.org/10.1016/S0749-0720(15)30982-8

Montesinos, E. (2003). Development, registration and commercialization of microbial pesticides for plant protection. *International Microbiology*, *6*, 245–252. https://doi.org/10.1007/s10123-003-0144-x

Murugesan, A. & Manoharan, M. (2020). Dengue virus. In M. M. Ennaji (Ed.), *Emerging and Reemerging Viral Pathogens* (pp. 281–359). Academic Press. https://doi.org/10.1016/B978-0-12-819400-3.00016-8

Noor, A. A. M. (2023). *Melaleuca cajuputi* Powell essential oil: A review of botanical, phytochemical and pharmacological properties. *Borneo Journal of Resource Science and Technology*, *13*(2), 1–12. https://doi.org/10.33736/bjrst.5314.2023

Noor, A. A. M., Yusuf, S. M., Wahab, W. N. A. W. A., Adam, M. F. I. C., & Sul'ain, M. D. (2021). Evaluation on composition, antioxidant and toxicity of *Melaleuca cajuputi* leaves. *Advances in Traditional Medicine*, *21*(4), 693–699. https://doi.org/10.1007/s13596-020-00479-x

O'Boyle, N. M., Banck, M., James, C. A., Morley, C., Vandermeersch, T., & Hutchison, GR. (2011). Open Babel: An open chemical toolbox. *Journal of Cheminformatics*, *3*(1), 33. https://doi.org/10.1186/1758-2946-3-33

Pettersen, E. F., Goddard, T. D., Huang, C. C., Meng, E. C., Couch, G. S., Croll, T. I., Morris, J. H., & Ferrin, T. E. (2021). UCSF ChimeraX: Structure visualization for researchers, educators, and developers. *Protein Science*, *30*(1), 70–82. https://doi.org/10.1002/pro.3943

Rizvi, S. M. D., Shakil, S. & Haneef, M. (2013). A simple click by click protocol to perform docking: AutoDock 4.2 made easy for non-bioinformaticians.*EXCLIJournal*,*12*:831–857. https://www.excli.de/excli/article/view/1196

Rizvi, S. M. D., Shakil, S. & Haneef, M. (2013). A simple click by click protocol to perform docking: AutoDock 4.2 made easy for non-bioinformaticians. *EXCLIJournal*,*12*:831–857. https://www.excli.de/excli/article/view/1196

Sierra, I., Latorre-Estivalis, J. M., Traverso, L., Gonzalez, P. V., Aptekmann, A., Nadra, A. D., Masuh, H., & Ons, S. (2021). Transcriptomic analysis and molecular docking reveal genes involved in the response of *Aedes aegypti* larvae to an essential oil extracted from *Eucalyptus*. *PLoS Neglected Tropical Diseases*, *15*(3), e0009587. https://doi.org/10.1371/journal.pntd.0009587

Su, T., & Mulla, M. S. (1999). Activity and biological effects of neem products against arthropods of medical and veterinary importance. *Journal of the American Mosquito Control Association*, *15*(2), 133–152. https://www.biodiversitylibrary.org/content/part/JAMCA/JAMCA_V15_N2_P133-152.pdf

Wahab, A. (2020). The outbreak of Covid-19 in Malaysia: Pushing migrant workers at the margin. *Social Sciences & Humanities Open*, *2*(1), 100073. https://doi.org/10.1016/j.ssaho.2020.100073

Waterhouse, A., Bertoni, M., Bienert, S., Studer, G., Tauriello, G., Gumienny, R., Heer, F. T., de Beer, T. A. P., Rempfer, C., & Bordoli, L. (2018). SWISS-MODEL: homology modelling of protein structures and complexes. *Nucleic Acids Research*, *46*(W1), W296–W303. https://doi.org/10.1093/nar/gky427

World Health Organization (2025). Dengue and severe dengue. World Health Organization. https://www.who.int/news-room/fact-sheets/detail/dengue-and-severe-dengue

Xue, R. D., Ali, A., & Barnard, D. R. (2003). Laboratory evaluation of toxicity of 16 insect repellents in aerosol sprays to adult mosquitoes. *Journal of the American Mosquito Control Association*, *19*(3), 271–274. https://www.biodiversitylibrary.org/content/part/JAMCA/JAMCA_V19_N3_P271-274.pdf

Yin, J., Choo, Y. -M., Duan, H., & Leal, W. S. (2015). Selectivity of odorant-binding proteins from the southern house mosquito tested against physiologically relevant ligands. *Frontiers in physiology*, *6*, 56. https://doi.org/10.3389/fphys.2015.00056

Citation:
Bin Aqeel, M., Naeem, T., Mat Sharani, S., Salleh, M. Z., Sul'ain, M. D., Khan, Z., & Abu Bakar, N. (2026). Computational identification of *Melaleuca cajuputi* essential oil compounds targeting *Aedes aegypti* odorant receptors. *Life Sciences, Medicine and Biomedicine*, *10*(1).
https://doi.org/10.28916/lsmb.10.1.2026.258

Life Sciences, Medicine and Biomedicine
ISSN: 2600-7207